Hindawi
Journal of Sensors
Volume 2024, Article ID 5581891, 14 pages
https://doi.org/10.1155/2024/5581891

Research Article

The Multisensor Data Fusion Method Based on Improved Fuzzy Evidence Theory in the Coal Mine Environment

Lei Wang[1], **Chenyan Fu**[1] **and Junyan Qi**[2]

[1]*School of Computer Science and Technology, Henan Polytechnic University, Jiaozuo, 454000, Henan, China*
[2]*School of Software, Henan Polytechnic University, Jiaozuo, 454000, Henan, China*

Correspondence should be addressed to Chenyan Fu; fcy@home.hpu.edu.cn

Received 21 September 2023; Revised 20 October 2023; Accepted 18 January 2024; Published 31 January 2024

Academic Editor: Carmine Granata

An enhanced evidence theory-based multisensor data fusion technique is presented to address the problem of poor data fusion caused by an unknown interference in the fully automated mining face multisensor system of a coal mine. Initially, the set of all measurement values is considered as the identification framework, and the principles of fuzzy mathematics are applied to introduce the membership function. This leads to the proposal of a novel method for calculating mutual support among multiple sensors. Furthermore, the basic belief assignment (BBA) in evidence theory is determined by measuring the confidence distance between sensors. Subsequently, a divergence measure is employed to assess the level of conflict and difference between BBA functions, which serves as an indicator of their credibility. The credibility of BBA functions is further adjusted by calculating their information volume using Shannon entropy. This adjustment aims to increase the weight of BBA functions that exhibit less conflict with other BBA functions. Ultimately, the fusion result is obtained through an evidence combination rule based on a conflict allocation. The numerical experimental results demonstrate that the proposed approach achieves higher accuracy, better robustness, and generality compared to the existing methods.

1. Introduction

To ensure the safe advancement of the coal mine comprehensive excavation workface, it is necessary to sense the dynamic information of equipment status and surrounding environment through a variety of sensors. Because of the ambiguity in describing the external environment by a single sensor, it cannot provide accurate information. Therefore, it is necessary to fuze data from multiple sensors to express the accurate information of the external environment.

To achieve effective fusion of multisensor data, scholars at home and abroad have conducted in-depth research. Li et al. [1] fuzed data from the different sensors based on an adaptive weighting algorithm which follows the principle of minimizing the total mean-squared error. The method determines the weighting factors by seeking the optimal solution and it is a relatively simple data fusion method. Yu [2] first uses the correlation function to remove the data with low-sensor support and then uses the least-squares method to fuze the remaining data. This algorithm can obtain a representative value through simple mathematical calculations. Chen et al. [3] constructed a weight neural network model with time difference as an input feature by introducing a compensation strategy based on the previous measurement update time to solve the asynchronous problem of the multisensor data. Other methods include batch estimation [4], genetic algorithm [5], particle filter algorithm [6], Kalman filter algorithm [7, 8], etc. Because of the complexity of the coal mining environment, limitations of sensors themselves, noise interference and human intervention, the information collected by the sensors is characterized by fuzziness, uncertainty, inconsistency, and incompleteness. However, none of the above-mentioned methods can solve the problem of uncertainty in the multisensor data fusion.

With more and more experts and scholars delving into the issue, mature theories have emerged to handle such uncertain information, among which the most commonly used are Bayesian theory [9, 10] and Dempster–Shafer evidence theory. However, Bayesian theory requires prior probability to be obtained before obtaining new probability,

which is not suitable for the real-time data fusion in comprehensive mining works. Evidence theory can express "uncertainty" and "unknown" of information through its defined basic belief assignment (BBA) function and likelihood function when prior probability is unknown, making it an excellent method for dealing with the uncertainty and incompleteness. The evidence theory has been widely applied and researched. For example, in order to effectively convert objective data from the real world into the BBA framework of evidence theory, Deng and Han [11] proposed a strong constraint general BBA method. This method constructs different triangular fuzzy number models based on the minimum, average, and maximum values of the different sample attributes, and determines the BBA by using the intersection points of the sample and different models. Tang et al. [12] utilizes Belief Jensen–Shannon (BJS) divergence to measure the level of conflict among experts and employs Deng entropy to assess the uncertainty of the risk factors in failure modes (FM). Finally, Dempster's combination rule is applied to generate a fuzed BBA for the three risk levels of the risk factors in FM. Wang and Tang [13] constructed a Gaussian distribution based on the mean and variance of the training samples in the data set, and generated the BBA by calculating the function value of the test sample on the Gaussian distribution. Fu et al. [14] constructed multiple strong classifiers through the Adaboost algorithm and recorded the corresponding weights for determining the BBA of singleton propositions and obtained the BBA of composite propositions by quantifying the cross-sectional area of singleton proposition intersections. In order to quantify the uncertainty of the BBA function, Pan et al. [15] proposed a new belief entropy based on likelihood transformation and weighted Hartley entropy. The first component of the entropy is used to measure the inconsistent uncertainty of the BBA, which not only considers the BBA, but also considers the likelihood transformation. The second component is used to measure the nonspecific uncertainty of the BBA. On the basis of Deng 's [16] entropy, Zhou et al. [17] proposed an improved belief entropy by considering the size of the identification frame and the information of the size of the focus element relative to the identification frame. Yan and Deng [18] introduced the belief function on the basis of Zhou, which solved the problem that different subsets interact with each other and are not measured. Zhu and Song [19] proposed a new measure of evidence uncertainty from the perspective of the credibility interval. They used the likelihood functions and the credibility functions as the upper and lower bounds of the credibility interval and used the inconsistency of the median calculation of the interval and the inaccuracy of the length calculation of the interval to combine the two to obtain an uncertainty measure. In order to overcome the counterintuitive results of highly contradictory evidence combination, Tang et al. [20] introduced the concept of a complex network, treating each body of evidence (BOE) as a node and employing correlation coefficients to measure the degree of correlation between two BOEs. Through direct and indirect interactions, the weights for each node were determined. These weights were then used to calculate the total weight for each BOE. In the end, the original BOEs were adjusted using weight factors, and the final result is obtained after information fusion by using Dempster's combination rule. Huang and Xiao [21] proposed a novel measure called the higher order BJS divergence, marking the first approach to dynamically measure the discrepancy between BBAs over the time evolution. Ma et al. [22] introduced the concept of complete conflict and proposed a flexible combination rule based on the Dempster combination rule and evidence weight. Xiao [23] proposed an evidence combination method based on the prospect theory and evidence credibility measure. Mi et al. [24] proposed a combination method based on the soft likelihood function and ordered weighted averaging operator. However, most of these methods are used for emergency decision [25], state estimation, and fault diagnosis and cannot fuze multisensor measurements. In order to realize the fusion of multisensor measurements, Xiong and Yang [26] proposed a new multisensor data fusion method. The method converts each measured value into corresponding BBA function according to its accuracy and the basic belief distribution of each measured value is recorded as the fusion weighting coefficient. Finally, the data fusion result can be obtained by weighted summation of the all measured values. In order to further improve the accuracy of data fusion results, this paper proposes an improved multisensor data fusion method. The main contributions of this study are summarized as follows:

(1) Treat all real-time measurements as an identification framework, calculate the inter-support degree among sensors, and combine it with the confidence distance between sensors to establish the BBA in evidence theory.
(2) A divergence measure is employed to assess the degree of conflict and difference between the BBA functions, which represents the credibility of a BBA function. The credibility of a BBA function is adjusted by calculating the information volume of a BBA function, which is used to allocate the weight of a BBA function.
(3) Based on the weights assigned to a BBA function, the BBA for all measured values is combined to produce the result of multisensor data fusion.

The organizational structure of this paper is as follows: Section 2 introduces the preliminary knowledge required for the proposed method. Section 3 introduces an improved multisensor data fusion method. In section 4, three comparative experiments between the proposed method and other data fusion methods are given. Section 5 gives the conclusion.

2. Preliminaries

2.1. Evidence Theory. As a mathematical method for dealing with uncertainty reasoning problems, the evidence theory has been widely applied in fields such as multiattribute decision-making [27, 28], information fusion [29, 30], target tracking [31, 32], and fault diagnosis [33, 34], due to its

flexibility and effectiveness in modeling uncertainty and inaccuracy without prior information.

Definition 1. Let Ω be a finite set of complete and mutually exclusive possible hypotheses, denoted by:

$$\Omega = \{\theta_1, \theta_2, \ldots, \theta_n\} , \tag{1}$$

where Ω is called the identification framework. The power set of 2^{Ω} is the identification framework, which is denoted as follows:

$$2^{\Omega} = \{\varnothing, \{\theta_1\}, \ldots, \{\theta_n\}, \ldots, \{\theta_1, \theta_2, \ldots, \theta_n\}, \Omega\}, \tag{2}$$

where $\varnothing$ represents the empty set.

Definition 2. For any proposition A in the identification framework Ω, a mapping $m: 2^{\Omega} \to [0, 1]$ is defined, which satisfies:

$$\begin{cases} \sum_{A \in 2^{\Omega}} m(A) = 1 \\ m(\varnothing) = 0 \end{cases} , \tag{3}$$

where m is called the BBA function, also known as the Mass function. If $m(A) > 0$, then A is called a focal element.

2.2. Shannon Entropy. In evidence theory, Shannon entropy is an effective method to measure the uncertainty or information volume of the BBA function.

Definition 3. Let m be a BBA function of the discernibility framework, A_i be a set of propositions of the discernibility framework, then the Shannon entropy $H(m)$ of m is expressed as follows:

$$H(m) = -\sum_i m(A_i) \log_2 m(A_i) , \tag{4}$$

where the larger the $H(m)$ of the BBA function, the more information volume the BBA function contains, indicating that other BBA functions support it more and the BBA function occupies a higher proportion in the final combination.

Shannon entropy satisfies the following properties:

(1) Nonnegativity, that is, $H(m) \geq 0$.
(2) Boundedness, that is, $0 \leq H(m) \leq \log_2(n)$; where n represents the number of elements in the identification framework.
(3) Determinacy, that is, $H(1, 0) = H(1, 0, 0) = H(1, 0, 0, 0) = \ldots = H(1, 0, \ldots, 0) = 0$. This property means that when a proposition A_i is fully supported, the BBA function has the least information volume.
(4) Symmetry, that is $H(m(A_1), m(A_2), \ldots, m(A_{2^{|\Omega|}})) = H(m(A_{2^{|\Omega|}}), \ldots, m(A_1))$; where can be any arrangement.

2.3. Belief Divergence Measure. Measuring the differences and conflicts between BBA functions has always been an unresolved issue in evidence theory, which is crucial for evidence synthesis [35]. In recent years, there have been many methods to measure the conflict of BBA functions, such as generalized evidential Jensen–Shannon (GEJS) divergence [36, 37], Jensen–Shannon (JS) divergence [38], BRE divergence [39], BJS divergence [40], etc. JS divergence requires the selection of appropriate parameters to quantify the differences and conflicts between BBAs. The selection of these parameters is influenced by subjective factors and improper selection of parameters will have a significant impact on the final data fusion results. BRE divergence is more complex in terms of calculation and implementation, requiring additional computational resources and time, particularly in practical applications of multisensor data fusion where real-time processing is required. BJS divergence emphasizes the mutual validation and support among sensors. This means that when multiple sensors observe the same phenomenon, BJS divergence can better account for the consistency and differences between these observations, thus enhancing the accuracy of data fusion. This is highly beneficial for improving monitoring and decision support of fully mined coal mine face. In summary, the proposed method adopts BJS divergence as a measure of BBA functions conflict.

Definition 4. Let m_1 and m_2 be two mutually exclusive BBA functions of the same identification framework and A_i be a set of propositions of the identification framework, then the BJS divergence between m_1 and m_2 is expressed as follows:

$$\begin{aligned} \mathrm{BJS}(m_1, m_2) &= \mathrm{H}\left(\frac{m_1 + m_2}{2}\right) - \frac{1}{2}H(m_1) - \frac{1}{2}H(m_2) \\ &= \frac{1}{2}\left[\sum_i m_1(A_i) \log_2\left(\frac{2m_1(A_i)}{m_1(A_i) + m_2(A_i)}\right)\right. \\ &\quad \left. + \sum_i m_2(A_i) \log_2\left(\frac{2m_2(A_i)}{m_1(A_i) + m_2(A_i)}\right)\right], \end{aligned} \tag{5}$$

where $\mathrm{H}(m_j) = -\sum_i m_j(A_i) \log_2 m_j(A_i)$ $(i = 1, 2, \ldots, n; j = 1, 2)$ represents Shannon entropy.

BJS divergence satisfies the following properties:

(1) Symmetry, that is, $\mathrm{BJS}(m_1, m_2) = \mathrm{BJS}(m_2, m_1)$.
(2) Boundedness, that is, $0 \leq \mathrm{BJS}(m_1, m_2) \leq 1$.
(3) Nondegeneracy, that is, $\mathrm{BJS}(m_1, m_2) = 0 \Leftrightarrow m_1 = m_2$.
(4) Triangular inequality, that is, $\mathrm{BJS}(m_1, m_2) + \mathrm{BJS}(m_2, m_3) \geq \mathrm{BJS}(m_1, m_3)$.

3. The Proposed Method

In the system, there are n sensors simultaneously measuring the target x, with the measurement value of the i-th sensor denoted as x_i $(i = 1, 2\ldots, n)$. Based on the theory of

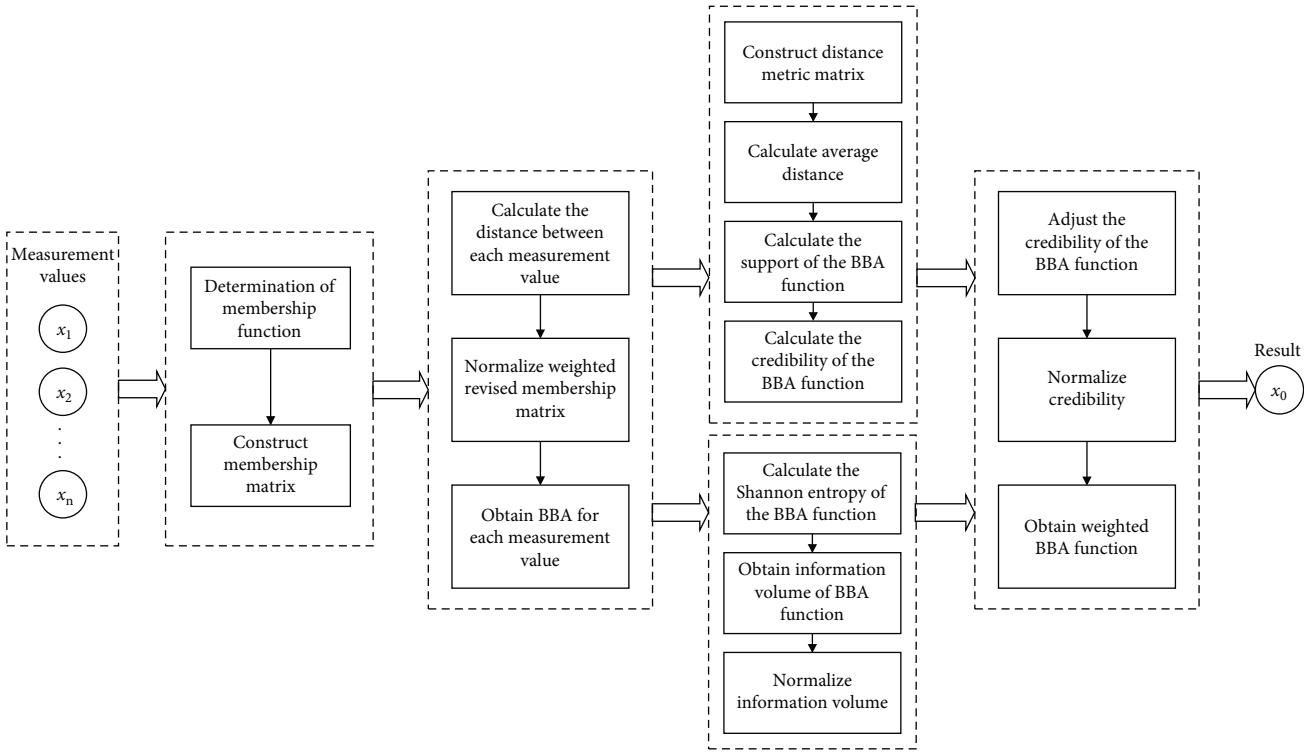

Figure 1: Flowchart of the proposed method.

evidence, all measurement values $\{x_1, x_2, \ldots, x_n\}$ are considered as the identification framework Ω and the BBA of each sensor's measurement value is calculated and then combined.

The proposed method consists of five parts: determination of membership function, BBA function of measurement value, quantify credibility of BBA function, quantify information volume of BBA function, and evidence combination. First, the membership function is determined and the membership matrix is constructed based on the distribution characteristics of the sensor measurement errors, reflecting the degree of support between each measurement value. Second, based on the membership matrix, the confidence distance between each measurement value, the average Euclidean distance from any measurement value to the other measurement values and the average distance between all measurement values are calculated. Based to the relationship between the ratio of BBA of measurement values and the ratio of distance, a set of weighting coefficients can be derived. The membership matrix is then normalized and weighted using these coefficients to obtain the BBA for each measurement value. Subsequently, the credibility of the BBA function is obtained by calculating the BJS divergence and the information volume of the BBA function is calculated by using Shannon entropy. After normalizing the information volume to be used as a weight, the credibility of the BBA function is adjusted, and then the adjusted credibility is normalized to obtain the final weight of the BBA function. Finally, the BBA function is combined according to this final weight to obtain the combination result. The flowchart of the proposed method is shown in Figure 1.

3.1. Determination of Membership Function. Because of the influence of environmental noise, human interference, and measurement inaccuracies, the sensor's measured value can be considered as the combination of the true target value and noise interference [35]. All measured values within the normal deviation range are typically distributed in the vicinity of the true value. Since the sensor measurement error is approximately normally distributed and the half-normal distribution function can better reflect the ambiguity of measurement value errors, the half-normal distribution function is selected as the membership function.

Definition 5. For any measurement value x_i $(i = 1, 2\ldots, n)$ in the identification framework Ω, the degree of membership of the measurement value x_j $(j = 1, 2\ldots, n)$ to that measurement value is defined as γ_{ij} and its mathematical expression is as follows:

$$\gamma_{ij} = \left(\frac{\pi}{2}\right)^{-\left(x_i - x_j\right)^2}, \tag{6}$$

where x_i and x_j represent the measurement values of the i-th and j-th sensors, respectively.

The larger the value of γ_{ij}, the higher the degree of support of x_j for x_i; Conversely, the lower the degree of support. For the identification framework Ω, the degree of membership matrix Γ composed of the degree of mutual support between each measurement value is expressed as follows:

$$\Gamma = \begin{bmatrix} \gamma_{11} & \gamma_{12} & \cdots & \gamma_{1n} \\ \gamma_{21} & \gamma_{22} & \cdots & \gamma_{2n} \\ \vdots & \vdots & \ddots & \vdots \\ \gamma_{n1} & \gamma_{n2} & \cdots & \gamma_{nn} \end{bmatrix} . \quad (7)$$

3.2. BBA Function of Measurement Value. Based on the membership matrix, let vector p_i $(i = 1, 2\ldots, n)$ be the i-th row of Γ, that is, $p_i = (\gamma_{i1}, \gamma_{i2}, \ldots, \gamma_{in})$, representing the membership degree vector of mutual support between the measurement values of the i-th sensor and the measurement values of the other sensors. Let d_{ij} represents the confidence distance from measurement value x_i to measurement value x_j. d_i represents the average value of the i-th row of d_{ij}. And $\overline{d}$ represents the average distance between the all measurement values. This is defined as follows:

$$d_{ij} = \|p_i - p_j\| = \sqrt{\sum_{k=1}^{n} (\gamma_{ik} - \gamma_{jk})^2} , \quad (8)$$

$$d_i = \frac{1}{n} \sum_{j=1}^{n} d_{ij} , \quad (9)$$

$$\overline{d} = \frac{1}{n} \sum_{i=1}^{n} d_i , \quad (10)$$

where the distance between any two measured values in Equation (8) is symmetrical, that is, $d_{ij} = d_{ji}$.

Measurement values within the normal deviation range should be clustered in the vicinity of the true value, while measurement values with large deviations are relatively far from the normal measurement values. Therefore, the following definitions are given.

Definition 6. All measurement values are located on the real axis and all normal measurement values are always distributed in a specific neighborhood near the true value. If the set φ satisfies the following conditions:

$$\begin{cases} d_i < \overline{d} (\forall x_i \in \varphi) \\ d_i \geq \overline{d} (\forall x_i \notin \varphi) \end{cases} , \quad (11)$$

where it is called the set of small deviation measurements for φ and the set of large deviation measurements for $\overline{\varphi}$. Here, $\overline{\varphi}$ represents the complement of φ, that is, $\varphi \cup \overline{\varphi} = \Omega$.

Taking into account the deviation level of the sensor measurements, the following method is provided to obtain the BBA for the sensor measurement value x_i.

(1) $\forall x_{i_1}, x_{i_1} \in \varphi$, the ratio of the obtained BBA is as follows:

$$\frac{m_k(x_{i_1})}{m_k(x_{i_2})} = \frac{d_{i_2}}{d_{i_1}} . \quad (12)$$

(2) $\forall x_i \in \varphi, x_j \in \overline{\varphi}$, the ratio of the obtained BBA is as follows:

$$\frac{m_k(x_i)}{m_k(x_j)} = \frac{d_{\max}}{d_{i_1}} , \quad (13)$$

$$d_{\max} = \max\{x_i\} - \min\{x_i\} , \quad (14)$$

where $\max\{x_i\}$ represents the maximum value in the sensor measurement and $\min\{x_i\}$ represents the minimum value in the sensor measurement.

During the computation phase, a series of weighting coefficients $\{w_p\}$ $(p = 1, 2, \ldots, n)$ can be generated using Equations (12)–(14). Using these coefficients, the membership matrix can be normalized and weighted, that is:

$$m_k(x_i) = \frac{w_j \times \gamma_{ij}}{\sum_{j=1}^{n} w_j \times \gamma_{ij}} . \quad (15)$$

At this point, the BBA for each sensor's measurement value is obtained and the conversion from measurement values to BBA functions is completed.

3.3. Quantify Credibility of BBA Function. By employing the BJS divergence to measure the difference and conflict degree between BBA functions, one can obtain the credibility of the BBA functions, which is used to represent their reliability. When a BBA function receives sufficient support from the other BBA functions, it has fewer conflicts with other BBA functions, so it should be given a higher weight. Conversely, when a BBA function does not receive support from other BBA functions, it is considered to have a higher conflict with other BBA functions, so it should be given a lower weight. The credibility $\mathrm{Crd}(m_k)$ of the BBA function m_k is calculated by the following four steps:

Step 1: The distance between BBA functions m_k $(k = 1, 2, \ldots, n)$ and m_t $(t = 1, 2, \ldots, n)$ is represented by $\mathrm{BJS}_{\mathrm{kt}}$. The BJS divergence measure-ment matrix, that is, the distance measurement matrix $\mathrm{DMM} = (\mathrm{BJS}_{\mathrm{kt}})_{n \times n}$ is defined as follows:

$$\mathrm{DMM} = \begin{bmatrix} 0 & \mathrm{BJS}_{12} & \cdots & \mathrm{BJS}_{1n} \\ \mathrm{BJS}_{21} & 0 & \cdots & \mathrm{BJS}_{2n} \\ \vdots & \vdots & \ddots & \vdots \\ \mathrm{BJS}_{n1} & \mathrm{BJS}_{n2} & \cdots & 0 \end{bmatrix} . \quad (16)$$

Step 2: The average distance $\widetilde{\mathrm{BJS}}(m_k)$ of the BBA function m_k is defined as follows:

Table 1: Roof pressure measurement values.

Number	Measurement value (MPa)	Number	Measurement value (MPa)
1	34.91	5	35.05
2	35.11	6	34.85
3	35.18	7	35.58
4	34.88	8	34.97

$$\widetilde{\mathrm{BJS}}(m_k) = \frac{\sum_{t=1,t\neq k}^{n} \mathrm{BJS}_{kt}}{n-1}. \tag{17}$$

Step 3: The support degree $\mathrm{Sup}(m_k)$ of the BBA function m_k is defined as follows:

$$\mathrm{Sup}(m_k) = \frac{1}{\widetilde{\mathrm{BJS}}(m_k)}. \tag{18}$$

Step 4: The credibility $\mathrm{Crd}(m_k)$ of BBA function m_k is defined as follows:

$$\mathrm{Crd}(m_k) = \frac{\mathrm{Sup}(m_k)}{\sum_{i=1}^{n} \mathrm{Sup}(m_k)}. \tag{19}$$

3.4. Quantify Information Volume of BBA Function. Shannon entropy is used to express the uncertainty of the BBA function, from which the information volume of the BBA function is calculated and normalized. The following three steps are used to calculate the normalized information volume $\widetilde{\mathrm{IV}}(m_k)$ for the BBA function m_k:

Step 1: Calculate the Shannon entropy $E(m_k)$ of the BBA function m_k by Equation (4).

Step 2: In order to avoid assigning a zero-value weight to the BBA function in special cases, the information volume IV is used to measure the uncertainty of the BBA function m_k. The information volume $\mathrm{IV}(m_k)$ of the BBA function m_k is defined as follows:

$$\mathrm{IV}(m_k) = \mathrm{e}^{\mathrm{E}(m_k)} = \mathrm{e}^{-\sum_i m_k(\mathrm{x}_i)\log_2 m_k(\mathrm{x}_i)}. \tag{20}$$

Step 3: Normalize $\mathrm{IV}(m_k)$ to obtain the normalized information volume $\widetilde{\mathrm{IV}}(m_k)$ of the BBA function m_k and denote it as follows:

$$\widetilde{\mathrm{IV}}(m_k) = \frac{\mathrm{IV}(m_k)}{\sum_{k=1}^{n} \mathrm{IV}(m_k)}. \tag{21}$$

3.5. Evidence Combination. The credibility of the BBA function is adjusted using the information volume of the BBA function to determine the final weight, and then the initial BBA function is combined. The steps to combine the initial BBA functions are as follows:

Step 1: Adjust the credibility $\mathrm{Crd}(m_k)$ of the BBA function based on the information volume $\mathrm{IV}(m_k)$ and denote it as $\mathrm{ACrd}(m_k)$:

$$\mathrm{ACrd}(m_k) = \mathrm{Crd}(m_k) \times \widetilde{\mathrm{IV}}(m_k). \tag{22}$$

Step 2: Normalize the adjusted credibility $\mathrm{ACrd}(m_k)$ to obtain the normalized credibility $\widetilde{\mathrm{ACrd}}(m_k)$ of the BBA function m_k, which serves as the final weight of the BBA function m_k. The normalized credibility $\widetilde{\mathrm{ACrd}}(m_k)$ is denoted as follows:

$$\widetilde{\mathrm{ACrd}}(m_k) = \frac{\mathrm{ACrd}(m_k)}{\sum_{k=1}^{n} \mathrm{ACrd}(m_k)}. \tag{23}$$

Step 3: According to the final weight $\widetilde{\mathrm{ACrd}}(m_k)$, obtain the weighted BBA function $m(x_i)$, denoted as follows:

$$m(x_i) = \sum_{k=1}^{n} \left(\widetilde{\mathrm{ACrd}}(m_k) \times m_k(x_i) \right). \tag{24}$$

Step 4: Obtain the combination value x_0 as follows:

$$x_0 = \sum_{i=1}^{n} (m(x_i) \times x_i). \tag{25}$$

4. Experiments

To demonstrate the universality and superiority of the proposed algorithm, two examples of single-sensor multiple measurements data fusion and one example of multisensor single measurement data fusion are provided to analyze the performance of the method.

4.1. Experiment 1. Fusion processing of roof pressure data for a comprehensive mining face. To evaluate the fusion accuracy of this method, roof pressure was measured 50 times, with an average value of 35.00 MPa serving as the reference. Eight measurement values were randomly selected from the 50 datas, as shown in Table 1. This method was used for the data fusion.

The membership matrix $\Gamma = (\gamma_{ij})_{\mathrm{n}\times\mathrm{n}}$ is constructed from Equation (7) as follows:

Table 2: BBA of roof pressure measurement values.

BBA	Measurement values							
	x_1	x_2	x_3	x_4	x_5	x_6	x_7	x_8
$m_1(x_i)$	0.1494	0.1394	0.1184	0.1406	0.1513	0.1272	0.0177	0.1560
$m_2(x_i)$	0.1470	0.1421	0.1223	0.1375	0.1526	0.1238	0.0197	0.1551
$m_3(x_i)$	0.1461	0.1431	0.1236	0.1364	0.1530	0.1226	0.0204	0.1548
$m_4(x_i)$	0.1498	0.1390	0.1178	0.1410	0.1510	0.1277	0.0175	0.1562
$m_5(x_i)$	0.1477	0.1413	0.1211	0.1384	0.1522	0.1248	0.0191	0.1554
$m_6(x_i)$	0.1502	0.1386	0.1172	0.1415	0.1508	0.1282	0.0172	0.1563
$m_7(x_i)$	0.1410	0.1484	0.1315	0.1302	0.1553	0.1157	0.0251	0.1527
$m_8(x_i)$	0.1487	0.1402	0.1196	0.1396	0.1517	0.1262	0.0183	0.1558

$$\Gamma = \begin{bmatrix} 1 & 0.9821 & \cdots & 0.9912 & \cdots & 0.9984 \\ 0.9821 & 1 & \cdots & 0.9984 & \cdots & 0.9912 \\ 0.9676 & 0.9978 & \cdots & 0.9924 & \cdots & 0.9803 \\ 0.9996 & 0.9764 & \cdots & 0.9870 & \cdots & 0.9963 \\ 0.9912 & 0.9984 & \cdots & 1 & \cdots & 0.9971 \\ 0.9984 & 0.9699 & \cdots & 0.9821 & \cdots & 0.9935 \\ 0.8165 & 0.9051 & \cdots & 0.8809 & \cdots & 0.8453 \\ 0.9984 & 0.9912 & \cdots & 0.9971 & \cdots & 1 \end{bmatrix}. \tag{26}$$

Using $\boldsymbol{d}$ to represent the vector composed of d_i, it can be obtained from Equations (8) to (10) that $\boldsymbol{d} = [0.1061, 0.1117, 0.1296, 0.1128, 0.1039, 0.1245, 0.3641, 0.1015]$, $\overline{d} = 0.1443$. According to Equation (11), $\varphi = \{x_i\}(i \neq 7)$, $\overline{\varphi} = \{x_7\}$. A set of weighted coefficients $\{w_p\} = \{0.1476, 0.1402, 0.1209, 0.1389, 0.1507, 0.1259, 0.0215, 0.1544\}$ is generated from Equations (12) to (14) and the BBA of roof pressure measurement values are normalized and modified through Equation (15), as shown in Table 2.

The distance metric matrix $\mathrm{DMM} = (\mathrm{BJS}_{ij})_{n\times n}$ is constructed from Equation (16) as follows and the credibility of the BBA function m_k calculated by from Equations (17) to (23) are shown in Table 3.

$$\mathrm{DMM} = \begin{bmatrix} 0 & 0.0001 & \cdots & 0.0001 & \cdots & 0.0000 \\ 0.0001 & 0 & \cdots & 0.0000 & \cdots & 0.0001 \\ 0.0002 & 0.0000 & \cdots & 0.0000 & \cdots & 0.0001 \\ 0.0000 & 0.0001 & \cdots & 0.0001 & \cdots & 0.0000 \\ 0.0001 & 0.0000 & \cdots & 0 & \cdots & 0.0000 \\ 0.0000 & 0.0002 & \cdots & 0.0001 & \cdots & 0.0000 \\ 0.0013 & 0.0006 & \cdots & 0.0008 & \cdots & 0.0011 \\ 0.0000 & 0.0001 & \cdots & 0.0000 & \cdots & 0 \end{bmatrix}. \tag{27}$$

The values of the weighted BBA function m_k calculated by Equation (24) are shown in Table 4.

The result $x_0 = 35.0024$ is obtained from Equation (25) and the fusion results of the proposed method and other methods are shown in Table 5. It can be seen from Table 5 that the fusion accuracy of the proposed method is higher. The higher accuracy of the fuzed results obtained by the proposed method is attributed to its utilization of BJS divergence and Shannon entropy to, respectively, assess the credibility and information content of BBA functions. This approach enhances the weights of reliable BBA functions while diminishing the weights of less reliable ones, leading to a more reasonable fusion outcome. To verify the robustness of the method, an experiment was conducted by adding a set of significantly large interference values to the sensor measurements. The fusion results of different methods on the roof pressure data are compared in Figure 2.

4.2. Experiment 2. Using a single sensor, dust concentration near the rear drum of the shearer was collected 50 times, and the average value of 1.406 g/m^3 was used as the reference value. Eight values were randomly selected from the 50 collected data as experimental data for data fusion using this method. The experimental data are shown in Table 6.

The membership matrix $\Gamma = (\gamma_{ij})_{\mathrm{n}\times\mathrm{n}}$ is constructed from Equation (7) as follows:

$$\Gamma = \begin{bmatrix} 1 & 0.8920 & \cdots & 0.9349 & \cdots & 0.9986 \\ 0.8920 & 1 & \cdots & 0.6998 & \cdots & 0.8688 \\ 0.9782 & 0.9647 & \cdots & 0.8467 & \cdots & 0.9662 \\ 0.9967 & 0.9245 & \cdots & 0.9043 & \cdots & 0.9911 \\ 0.9349 & 0.6998 & \cdots & 1 & \cdots & 0.9517 \\ 0.8532 & 0.5813 & \cdots & 0.9808 & \cdots & 0.8775 \\ 0.9776 & 0.7877 & \cdots & 0.9882 & \cdots & 0.9872 \\ 0.9986 & 0.8688 & \cdots & 0.9517 & \cdots & 1 \end{bmatrix}. \tag{28}$$

Using $\boldsymbol{d}$ to represent the vector composed of d_i, it can be obtained from Equations (8) to (10) that $\boldsymbol{d} = [0.2136, 0.4467, 0.2702, 0.2261, 0.2938, 0.4250, 0.2405, 0.2144]$, $\overline{d} = 0.2913$. According to Equation (11), $\varphi = \{x_1, x_3, x_4, x_7, x_8\}$, $\overline{\varphi} = \{x_2, x_5, x_6\}$. A set of weighted coefficients $\{w_p\} = \{0.1921,$

Table 3: Credibility of the BBA function for the roof pressure measurements.

BBA function	$\widetilde{\mathrm{BJS}}(m_k)$	$\mathrm{Sup}(m_k)$	$\mathrm{Crd}(m_k)$	$\boldsymbol{E}(m_k)$	$\mathrm{IV}(m_k)$	$\widetilde{\mathrm{IV}}(m_k)$	$\mathrm{ACrd}(m_k)$	$\widetilde{\mathrm{ACrd}}(m_k)$
m_1	0.0002	4,239.8915	0.1212	2.8803	17.8202	0.1244	0.0151	0.1208
m_2	0.0002	6,101.2474	0.1745	2.8864	17.9292	0.1252	0.0218	0.1749
m_3	0.0002	5,055.3676	0.1446	2.8885	17.9664	0.1254	0.0181	0.1452
m_4	0.0003	3,736.3295	0.1068	2.8794	17.8035	0.1243	0.0133	0.1064
m_5	0.0002	6,268.3118	0.1792	2.8846	17.8969	0.1250	0.0224	0.1794
m_6	0.0003	3,281.0770	0.0938	2.8784	17.7867	0.1242	0.0117	0.0933
m_7	0.0010	984.1100	0.0281	2.8997	18.1680	0.1269	0.0036	0.0286
m_8	0.0002	5,304.9868	0.1517	2.8822	17.8533	0.1247	0.0189	0.1514

Table 4: Weighted BBA function of the roof pressure measurements.

Measurement values	$m(x_i)$	Measurement values	$m(x_i)$
x_1	0.1480	x_5	0.1520
x_2	0.1410	x_6	0.1252
x_3	0.1207	x_7	0.0189
x_4	0.1387	x_8	0.1555

Table 5: Fusion results of different methods on roof pressure.

Method	Fusion result (MPa)	Absolute error (MPa)	Relative error (%)
Arithmetic mean	35.0663	0.0663	0.1894
Xiong and Yang [26]	34.9944	0.0056	0.0160
Qu et al. [41]	34.9918	0.0082	0.0234
Proposed method	35.0024	0.0024	0.0069

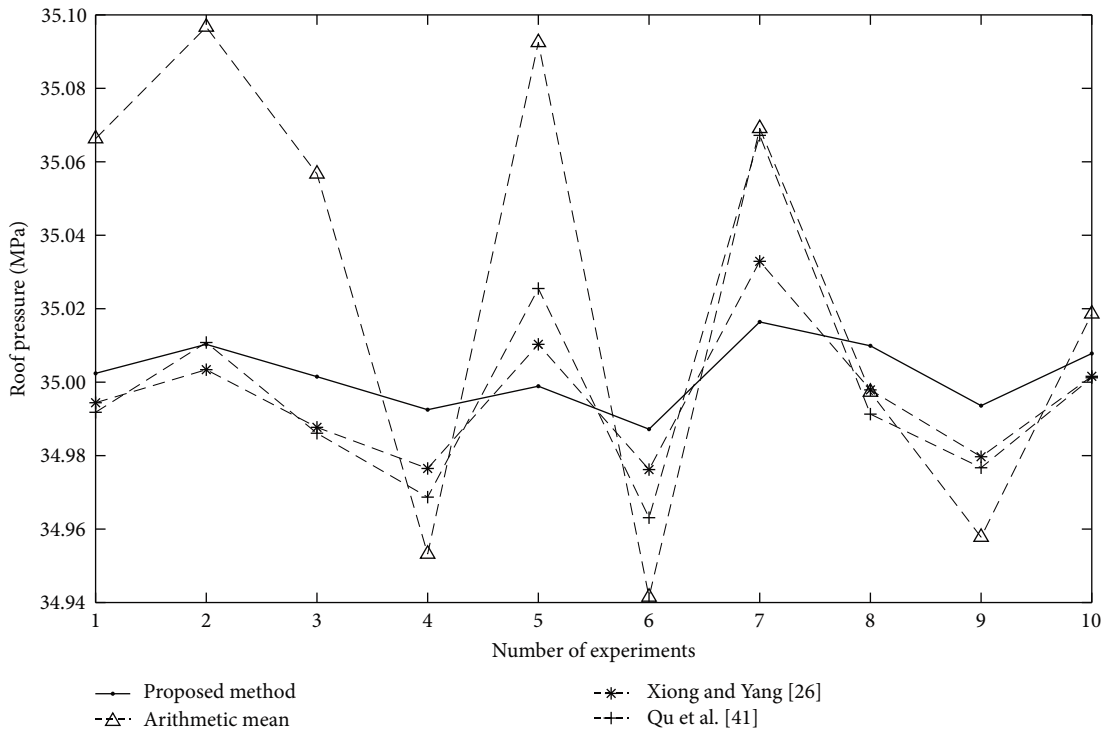

Figure 2: Comparison chart of roof pressure data fusion results.

Table 6: Dust concentration measurement values.

Number	Measurement value (g/m^3)	Number	Measurement value (g/m^3)
1	1.431	5	1.045
2	1.934	6	0.838
3	1.652	7	1.207
4	1.517	8	1.376

Table 7: BBA of dust concentration measurement values.

BBA	Measurement values							
	x_1	x_2	x_3	x_4	x_5	x_6	x_7	x_8
$m_1(x_i)$	0.1961	0.0341	0.1516	0.1846	0.0357	0.0326	0.1703	0.1950
$m_2(x_i)$	0.1966	0.0430	0.1681	0.1925	0.0301	0.0250	0.1542	0.1907
$m_3(x_i)$	0.1965	0.0378	0.1588	0.1882	0.0332	0.0290	0.1632	0.1933
$m_4(x_i)$	0.1963	0.0355	0.1544	0.1860	0.0347	0.0312	0.1675	0.1944
$m_5(x_i)$	0.1945	0.0284	0.1393	0.1777	0.0405	0.0398	0.1826	0.1972
$m_6(x_i)$	0.1932	0.0257	0.1328	0.1738	0.0433	0.0441	0.1892	0.1980
$m_7(x_i)$	0.1953	0.0307	0.1444	0.1807	0.0385	0.0366	0.1774	0.1964
$m_8(x_i)$	0.1959	0.0332	0.1498	0.1837	0.0364	0.0335	0.1720	0.1954

Table 8: Credibility of the BBA function for the dust concentration measurements.

BBA function	$\widetilde{\mathrm{BJS}}(m_k)$	$\mathrm{Sup}(m_k)$	$\mathrm{Crd}(m_k)$	$\boldsymbol{E}(m_k)$	$\mathrm{IV}(m_k)$	$\widetilde{\mathrm{IV}}(m_k)$	$\mathrm{ACrd}(m_k)$	$\widetilde{\mathrm{ACrd}}(m_k)$
m_1	0.0008	1,273.9942	0.1870	2.7172	15.1378	0.1249	0.0234	0.1868
m_2	0.0030	333.5024	0.0490	2.7031	14.9253	0.1231	0.0060	0.0482
m_3	0.0013	758.6873	0.1114	2.7112	15.0475	0.1241	0.0138	0.1106
m_4	0.0009	1,099.4713	0.1614	2.7149	15.1033	0.1246	0.0201	0.1609
m_5	0.0015	645.3294	0.0947	2.7267	15.2820	0.1261	0.0119	0.0955
m_6	0.0029	348.5009	0.0512	2.7312	15.3511	0.1266	0.0065	0.0518
m_7	0.0010	1,038.8645	0.1525	2.7229	15.2237	0.1256	0.0192	0.1532
m_8	0.0008	1,313.9660	0.1929	2.7186	15.1594	0.1250	0.0241	0.1930

$0.0374, 0.1519, 0.1815, 0.0374, 0.0374, 0.1706, 0.1914\}$ is generated from Equations (12) to (14) and the BBA of the dust concentration measurement values are normalized and modified through Equation (15), as shown in Table 7.

The distance metric matrix $\mathrm{DMM} = (\mathrm{BJS}_{ij})_{n\times n}$ is constructed from Equation (16) as follows and the credibility of the BBA function m_k calculated by from Equations (17) to (23) are shown in Table 8.

$$\mathrm{DMM} = \begin{bmatrix} 0 & 0.0016 & \cdots & 0.0010 & \cdots & 0.0000 \\ 0.0016 & 0 & \cdots & 0.0050 & \cdots & 0.0019 \\ 0.0003 & 0.0005 & \cdots & 0.0023 & \cdots & 0.0005 \\ 0.0000 & 0.0011 & \cdots & 0.0014 & \cdots & 0.0001 \\ 0.0010 & 0.0050 & \cdots & 0 & \cdots & 0.0007 \\ 0.0023 & 0.0076 & \cdots & 0.0003 & \cdots & 0.0019 \\ 0.0003 & 0.0033 & \cdots & 0.0002 & \cdots & 0.0002 \\ 0.0000 & 0.0019 & \cdots & 0.0007 & \cdots & 0 \end{bmatrix}. \tag{29}$$

The values of the weighted BBA function m_k calculated by Equation (24) are shown in Table 9.

The result $x_0 = 1.4135$ is obtained from Equation (25) and the fusion results of the proposed method with other methods are shown in Table 10. From Table 10, it can be seen that the proposed method has higher fusion accuracy. Due to the fact that the proposed method does not exclude anomalous measurement values in the final evidence combination, the fuzed results exhibit higher credibility. The robustness experimental results of different methods on the dust concentration data are shown in Figure 3.

4.3. Experiment 3. By measuring the angles with eight inclination sensors installed in different positions, the height of the hydraulic support can be calculated. Each sensor measures five times, resulting in 40 measurements. Eight of these measurements are randomly selected for data fusion and the average of the forty measurements, which is 623.00 mm, is used as a reference. The experimental data are shown in Table 11.

Table 9: Weighted BBA function of the dust concentration measurements.

Measurement values	$m(x_i)$	Measurement values	$m(x_i)$
x_1	0.1957	x_5	0.0364
x_2	0.0335	x_6	0.0337
x_3	0.1501	x_7	0.1719
x_4	0.1836	x_8	0.1952

Table 10: Fusion results of different methods on dust concentration.

Method	Fusion result (g/m^3)	Absolute error (g/m^3)	Relative error (%)
Arithmetic mean	1.3750	0.0310	2.2048
Xiong and Yang [26]	1.4184	0.0124	0.8819
Qu et al. [41]	1.4296	0.0236	1.6785
Proposed method	1.4135	0.0075	0.5334

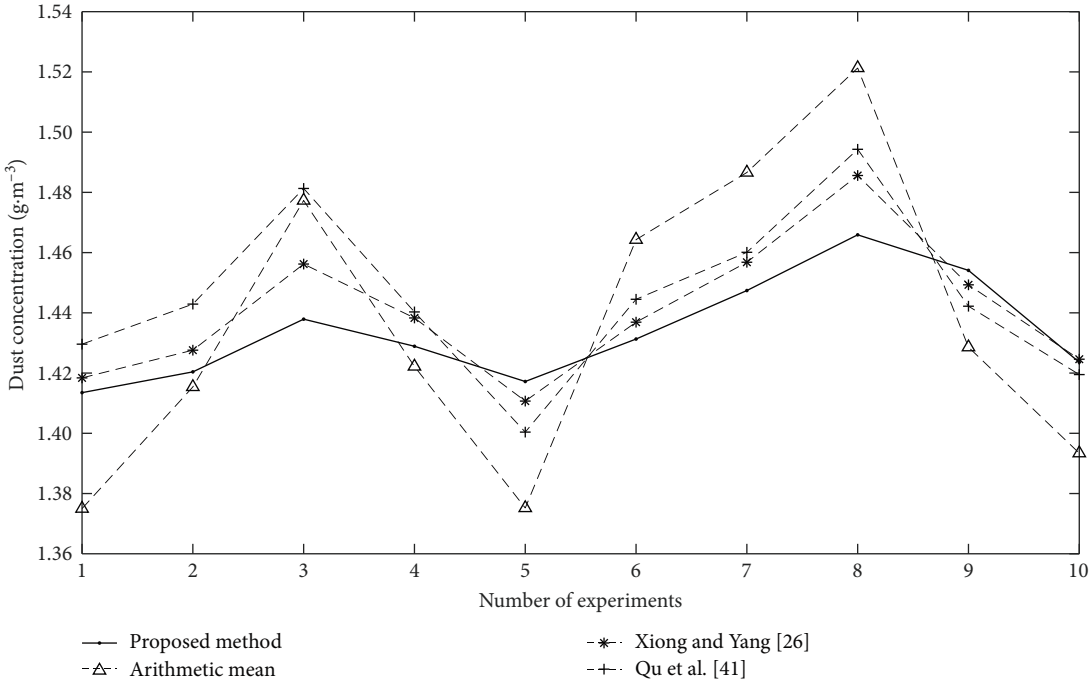

Figure 3: Comparison chart of dust concentration data fusion results.

The membership matrix $\Gamma = (\gamma_{ij})_{n\times n}$ is constructed from Equation (7) as follows:

$$\Gamma = \begin{bmatrix} 1 & 0.9210 & \cdots & 0.8834 & \cdots & 0.9830 \\ 0.9210 & 1 & \cdots & 0.6647 & \cdots & 0.8397 \\ 0.7447 & 0.9366 & \cdots & 0.4488 & \cdots & 0.6349 \\ 0.9741 & 0.9845 & \cdots & 0.7678 & \cdots & 0.9177 \\ 0.8834 & 0.6647 & \cdots & 1 & \cdots & 0.9523 \\ 0.5549 & 0.3290 & \cdots & 0.8416 & \cdots & 0.6670 \\ 0.7662 & 0.5247 & \cdots & 0.9735 & \cdots & 0.8622 \\ 0.9830 & 0.8397 & \cdots & 0.9523 & \cdots & 1 \end{bmatrix}. \quad (30)$$

Using $\boldsymbol{d}$ to represent the vector composed of d_i, it can be obtained from Equations (8) to (10) that $\boldsymbol{d} = [0.5658, 0.6854, 0.9175, 0.6115, 0.6397, 0.9893, 0.7448, 0.5686]$, $\overline{d} = 0.7153$. According to Equation (11), $\varphi = \{x_1, x_2, x_4, x_5, x_8\}$, $\overline{\varphi} = \{x_3, x_6, x_7\}$. A set of weighted coefficients $\{w_p\} = \{0.1818, 0.1501, 0.0528, 0.1682, 0.1608, 0.0528, 0.0528, 0.1809\}$ is generated from Equations (12) to (14) and the BBA of the hydraulic support height measurement values are normalized and modified through Equation (15), as shown in Table 12.

The distance metric matrix $\mathrm{DMM} = (\mathrm{BJS}_{ij})_{n\times n}$ is constructed from Equation (16) as follows and the credibility of the BBA function m_k calculated by from Equations (17) to (23) are shown in Table 13.

Table 11: Hydraulic support height measurement values.

Number	Measurement value (mm)	Number	Measurement value (mm)
1	622.928	5	623.452
2	622.501	6	624.070
3	622.120	7	623.696
4	622.687	8	623.123

Table 12: BBA of hydraulic support height measurement values.

BBA	Measurement values							
	x_1	x_2	x_3	x_4	x_5	x_6	x_7	x_8
$m_1(x_i)$	0.1992	0.1514	0.0430	0.1795	0.1556	0.0321	0.0443	0.1948
$m_2(x_i)$	0.2002	0.1795	0.0591	0.1980	0.1278	0.0208	0.0331	0.1816
$m_3(x_i)$	0.1968	0.2044	0.0767	0.2115	0.1049	0.0138	0.0250	0.1670
$m_4(x_i)$	0.2004	0.1672	0.0516	0.1903	0.1397	0.0252	0.0377	0.1879
$m_5(x_i)$	0.1907	0.1185	0.0281	0.1534	0.1910	0.0527	0.0610	0.2046
$m_6(x_i)$	0.1713	0.0838	0.0161	0.1204	0.2298	0.0896	0.0841	0.2049
$m_7(x_i)$	0.1842	0.1041	0.0227	0.1405	0.2070	0.0655	0.0698	0.2063
$m_8(x_i)$	0.1970	0.1389	0.0369	0.1701	0.1688	0.0388	0.0501	0.1994

Table 13: Credibility of the BBA function for the hydraulic support height measurements.

BBA function	$\widetilde{\mathrm{BJS}}(m_k)$	$\mathrm{Sup}(m_k)$	$\mathrm{Crd}(m_k)$	$\boldsymbol{E}(m_k)$	$\mathrm{IV}(m_k)$	$\widetilde{\mathrm{IV}}(m_k)$	$\mathrm{ACrd}(m_k)$	$\widetilde{\mathrm{ACrd}}(m_k)$
m_1	0.0120	83.0551	0.1886	2.7519	15.6727	0.1257	0.0237	0.1889
m_2	0.0211	47.4925	0.1079	2.7181	15.1509	0.1215	0.0131	0.1044
m_3	0.0370	27.0459	0.0614	2.6784	14.5617	0.1168	0.0072	0.0572
m_4	0.0159	62.8659	0.1428	2.7343	15.3990	0.1235	0.0176	0.1405
m_5	0.0155	64.5276	0.1466	2.7747	16.0340	0.1286	0.0189	0.1502
m_6	0.0419	23.8409	0.0541	2.7677	15.9226	0.1277	0.0069	0.0551
m_7	0.0230	43.4939	0.0988	2.7768	16.0680	0.1289	0.0127	0.1014
m_8	0.0114	87.9685	0.1998	2.7631	15.8483	0.1271	0.0254	0.2023

Table 14: Weighted BBA function of the hydraulic support height measurements.

Measurement values	$m(x_i)$	Measurement values	$m(x_i)$
x_1	0.1945	x_5	0.1648
x_2	0.1436	x_6	0.0399
x_3	0.0408	x_7	0.0496
x_4	0.1718	x_8	0.1950

$$\mathrm{DMM} = \begin{bmatrix} 0 & 0.0047 & \cdots & 0.0076 & \cdots & 0.0010 \\ 0.0047 & 0 & \cdots & 0.0240 & \cdots & 0.0101 \\ 0.0163 & 0.0035 & \cdots & 0.0451 & \cdots & 0.0253 \\ 0.0015 & 0.0009 & \cdots & 0.0158 & \cdots & 0.0051 \\ 0.0076 & 0.0240 & \cdots & 0 & \cdots & 0.0030 \\ 0.0367 & 0.0660 & \cdots & 0.0113 & \cdots & 0.0257 \\ 0.0164 & 0.0381 & \cdots & 0.0017 & \cdots & 0.0093 \\ 0.0010 & 0.0101 & \cdots & 0.0030 & \cdots & 0 \end{bmatrix}. \tag{31}$$

The values of the weighted BBA function m_k calculated by Equation (24) are shown in Table 14.

The result $x_0 = 623.0003$ is obtained from Equation (25) and the fusion results of the proposed method with other methods are shown in Table 15. From Table 15, it can be seen that the proposed method has higher fusion accuracy. Through three comparative experiments with other data fusion methods, it has been demonstrated that the proposed approach exhibits high levels of accuracy, generality, and robustness. The robustness experimental results of different

Table 15: Fusion results of different methods on hydraulic support height.

Method	Fusion result (mm)	Absolute error (mm)	Relative error (%)
Arithmetic mean	623.0721	0.0721	0.0116
Xiong and Yang [26]	622.9730	0.0270	0.0043
Qu et al. [41]	622.9648	0.0352	0.0057
Proposed method	623.0003	0.0003	0.0001

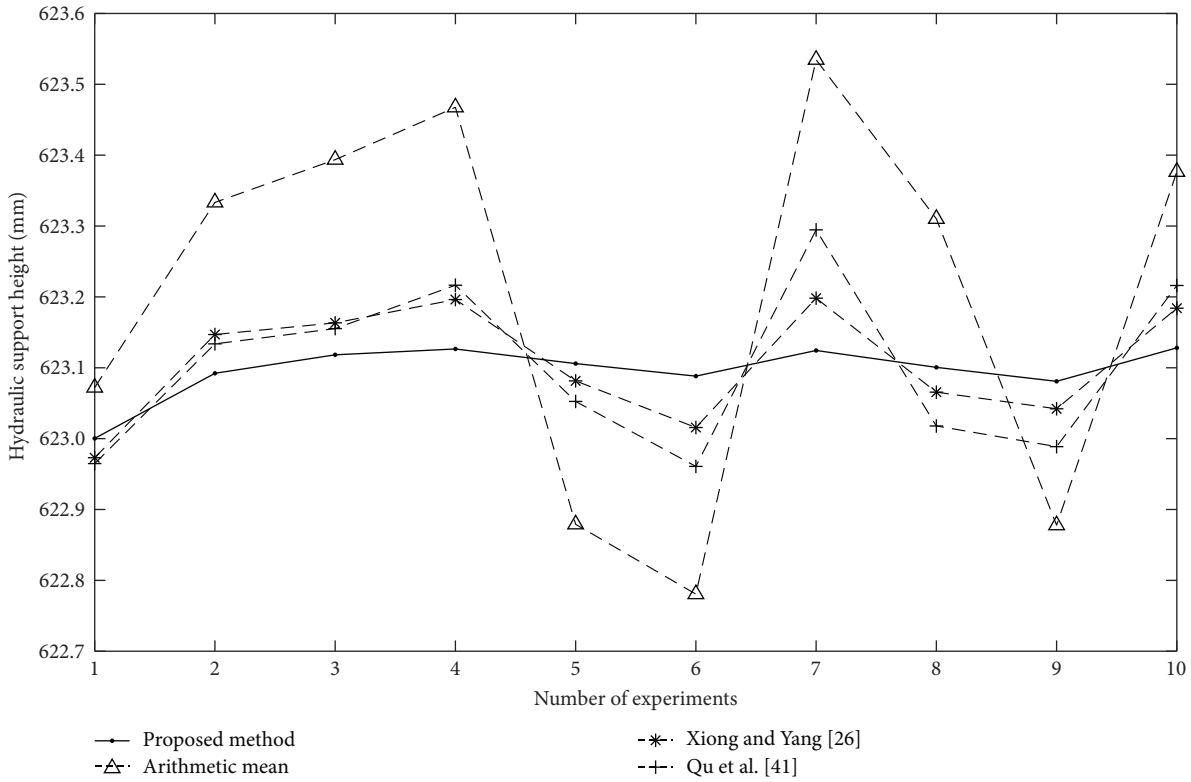

Figure 4: Comparison chart of hydraulic support height data fusion results.

methods on the hydraulic support height data are shown in Figure 4.

5. Conclusion and Future Work

To solve the problem of poor fusion accuracy caused by the uncertainty of real-time measurement values in the process of multisensor data fusion, an improved evidence theory-based multisensor data fusion method is proposed. By introducing membership functions and measuring confidence distances between sensors, the BBA in evidence theory is determined. The BJS divergence is used to assess the conflict and difference between BBA functions, generating the credibility of BBA functions to represent their reliability. Then, Shannon entropy is employed to calculate the information volume of BBA functions, providing an indication of their relative importance. Based on the information content, the credibility of BBA functions is adjusted to calculate the final weights for evidence combination, resulting in effective fusion results. The experimental results demonstrate that the method proposed in this paper can achieve higher fusion accuracy with relatively fewer measurement data, without the need for obtaining prior information of the sensors through historical data. This approach is beneficial for engineering implementation and can be applied to multisensor data fusion in fully mechanized mining faces in coal mines. Given that the proposed method is built on the principles of evidence theory, future research will primarily concentrate on achieving more precise measurements of the mutual support degree between sensors and its conversion into BBA functions. Additionally, there will be a focus on adjusting the evidence combination rules based on the inconsistency degree between BBA functions, with the aim of further enhancing the fusion performance of the algorithm.

Data Availability

The data used to support the findings of this study are available from the corresponding author upon request.

Conflicts of Interest

The authors declare that they have no conflicts of interest.

Acknowledgments

This work is supported by the Program for Innovative Research Team (in Science and Technology) in University of Henan Province (22IRTSTHN005).

References

[1] D. Li, C. Shen, X. Dai et al., "Research on data fusion of adaptive weighted multi-source sensor," *Computers, Materials & Continua*, vol. 61, no. 3, pp. 1217–1231, 2019.

[2] L. Yu, "Tunnel fire monitoring and alarm technology based on multi-sensor data fusion," *Tunnel Construction*, vol. 42, pp. 261–266, 2022.

[3] B. Chen, K. Yue, R. Wang, and M. Hu, "Learning-based multi-rate multi-sensor fusion localization method," *Acta Aeronautica et Astronautica Sinica*, vol. 43, pp. 43–52, 2022.

[4] S. Cao and Y. Liu, "Multi-sensor data fusion algorithm based on aquatic product live transporta-tion," *Journal of Shandong Agricultural University (Natural Science Edition)*, vol. 49, no. 6, pp. 941–545, 2018.

[5] G. Sun, Z. Zhang, B. Zheng, and Y. Li, "Multi-sensor data fusion algorithm based on trust degree and improved genetics," *Sensors*, vol. 19, no. 9, Article ID 2139, 2019.

[6] W. Chen, J. Chen, C. Zhang, L. Song, and Z. Tan, "Multisensor information fusion algorithm based on intelligent particle filtering," *Journal of Computer Applications*, vol. 36, no. 12, pp. 3358–3362, 2016.

[7] X. Liu, B. Zhou, P. Huang et al., "Kalman filter-based data fusion of Wi-Fi RTT and PDR for indoor localization," *IEEE Sensors Journal*, vol. 21, no. 6, pp. 8479–8490, 2021.

[8] F. Liu, Y. Liu, X. Sun, and H. Sang, "A new multi-sensor hierarchical data fusion algorithm based on unscented Kalman filter for the attitude observation of the wave glider," *Applied Ocean Research*, vol. 109, Article ID 102562, 2021.

[9] W. Yang, B. Chen, and L. Yu, "Bayesian-wavelet-based multisource decision fusion," *IEEE Transactions on Instrumentation and Measurement*, vol. 70, pp. 1–10, 2021.

[10] N. Yu, Y. Sun, and H. Chen, "Prediction method of cutting loads of shearers based on multi-source data fusion," *China Mechanical Engineering*, vol. 32, no. 10, pp. 1247–1253, 1259, 2021.

[11] Y. Deng and D. Han, "Methods to determine generalized basic probability assignment in generalized evidence theory," *Journal of Xi'an Jiaotong University*, vol. 45, no. 2, Article ID 0034, 2011.

[12] Y. Tang, S. Tan, and D. Zhou, "An improved failure mode and effects analysis method using belief Jensen–Shannon divergence and entropy measure in the evidence theory," *Arabian Journal for Science and Engineering*, vol. 48, no. 5, pp. 7163–7176, 2023.

[13] S. Wang and Y. Tang, "An improved approach for generation of a basic probability assignment in the evidence theory based on Gaussian distribution," *Arabian Journal for Science and Engineering*, vol. 47, no. 2, pp. 1595–1607, 2022.

[14] W. Fu, S. Yu, and X. Wang, "A novel method to determine basic probability assignment based on Adaboost and its application in classification," *Entropy*, vol. 23, no. 7, Article ID 812, 2021.

[15] Q. Pan, D. Zhou, Y. Tang, X. Li, and J. Huang, "A novel belief entropy for measuring uncertainty in Dempster–Shafer evidence theory framework based on plausibility transformation and weighted hartley entropy," *Entropy*, vol. 21, no. 2, Article ID 163, 2019.

[16] Y. Deng, "Deng entropy," *Chaos, Solitons & Fractals*, vol. 91, pp. 549–553, 2016.

[17] D. Zhou, Y. Tang, W. Jiang, and Y. Shi, "A modified belief entropy in Dempster–Shafer framework," *PLOS ONE*, vol. 12, no. 5, Article ID e0176832, 2017.

[18] H. Yan and Y. Deng, "An improved belief entropy in evidence theory," *IEEE Access*, vol. 8, pp. 57505–57516, 2020.

[19] Z. Zhu and Y. Song, "Uncertainty measure in evidence theory based on interval probability," *Journal of Computer Applications*, vol. 41, pp. 25–30, 2021.

[20] Y. Tang, G. Dai, Y. Zhou, Y. Huang, and D. Zhou, "Conflicting evidence fusion using a correlation coefficient-based approach in complex network," *Chaos, Solitons & Fractals*, vol. 176, Article ID 114087, 2023.

[21] Y. Huang and F. Xiao, "Higher order belief divergence with its application in pattern classification," *Information Sciences*, vol. 635, pp. 1–24, 2023.

[22] W. Ma, Y. Jiang, and X. Luo, "A flexible rule for evidential combination in Dempster–Shafer theory of evidence," *Applied Soft Computing*, vol. 85, Article ID 105512, 2019.

[23] F. Xiao, "Evidence combination based on prospect theory for multi-sensor data fusion," *ISA Transactions*, vol. 106, pp. 253–261, 2020.

[24] X. Mi, T. Lv, Y. Tian, and B. Kang, "Multi-sensor data fusion based on soft likelihood functions and OWA aggregation and its application in target recognition system," *ISA Transactions*, vol. 112, pp. 137–149, 2021.

[25] L. Fei and Y. Wang, "An optimization model for rescuer assignments under an uncertain environment by using Dempster–Shafer theory," *Knowledge-Based Systems*, vol. 255, Article ID 109680, 2022.

[26] Y. Xiong and Z. Yang, "Data fusion algorithm inspired by evidence theory," *Journal of Huazhong University of Science and Technology (Nature Science Edition)*, vol. 39, no. 10, pp. 50–54, 2011.

[27] F. Ye, J. Chen, Y. Li, and J. Kang, "Decision-making algorithm for multisensor fusion based on grey relation and DS evidence theory," *Journal of Sensors*, vol. 2016, Article ID 3954573, 11 pages, 2016.

[28] L. Fei and Y. Feng, "Modeling interactive multiattribute decision-making via probabilistic linguistic term set extended by Dempster–Shafer theory," *International Journal of Fuzzy Systems*, vol. 23, no. 2, pp. 599–613, 2021.

[29] Y. Zhang, A. Xiong, Y. Xiao, and Z. Chen, "A new combination method based on Pearson coefficient and information entropy for multi-sensor data fusion," *Information and Software Technology*, vol. 161, Article ID 107248, 2023.

[30] X. Fan, Y. Guo, Y. Ju, J. Bao, and W. Lyu, "Multisensor fusion method based on the belief entropy and DS evidence theory," *Journal of Sensors*, vol. 2020, Article ID 7917512, 16 pages, 2020.

[31] J. Li, X. Liu, Z. Wang et al., "Real-time hand gesture tracking for human–computer interface based on multi-sensor data fusion," *IEEE Sensors Journal*, vol. 21, no. 23, pp. 26642–26654, 2021.

[32] D.-C. Chang and Y.-C. Chang, "Investigation of weighted least squares methods for multitarget tracking with multisensor data fusion," *Journal of Signal Processing Systems*, vol. 95, no. 11, pp. 1311–1325, 2023.

[33] X. Yao, S. Li, and J. Hu, "Improving rolling bearing fault diagnosis by DS evidence theory based fusion model," *Journal of Sensors*, vol. 2017, Article ID 6737295, 14 pages, 2017.

[34] F. Zou, M. Jiang, X. Li et al., "Research on mechanical fault diagnosis based on MADS evidence fusion theory,"

Measurement Science and Technology, vol. 34, no. 8, Article ID 085901, 2023.

[35] S. Qiao, Y. Fan, G. Wang, and H. Zhang, "Multi-sensor data fusion method based on improved evidence theory," *Journal of Marine Science and Engineering*, vol. 11, no. 6, Article ID 1142, 2023.

[36] F. Xiao, Z. Cao, and C.-T. Lin, "A complex weighted discounting multisource information fusion with its application in pattern classification," *IEEE Transactions on Knowledge and Data Engineering*, vol. 35, no. 8, pp. 7609–7623, 2023.

[37] F. Xiao, J. Wen, and W. Pedrycz, "Generalized divergence-based decision making method with an application to pattern classification," *IEEE Transactions on Knowledge and Data Engineering*, vol. 35, no. 7, pp. 6941–6956, 2023.

[38] J. Lin, "Divergence measures based on the shannon entropy," *IEEE Transactions on Information Theory*, vol. 37, no. 1, pp. 145–151, 1991.

[39] Y. Song and Y. Deng, "A new method to measure the divergence in evidential sensor data fusion," *International Journal of Distributed Sensor Networks*, vol. 15, no. 4, 2019.

[40] F. Xiao, "Multi-sensor data fusion based on the belief divergence measure of evidences and the belief entropy," *Information Fusion*, vol. 46, pp. 23–32, 2019.

[41] J. Qu, S. Li, and C. Zhang, "Multi-sensor data fusion algorithm based on fuzzy evidence theory," *Instrument Technique and Sensor*, vol. 417, no. 10, pp. 118–122, 2017.